J|A|C|S
ARTICLES
Published on Web 09/22/2005

Interstrand and Intrastrand DNA−DNA Cross-Linking by 1,2,3,4-Diepoxybutane: Role of Stereochemistry

Soobong Park,[†] Christopher Anderson,[†] Rachel Loeber,[†] Mahadevan Seetharaman,[†] Roger Jones,[‡] and Natalia Tretyakova*,[†]

Contribution from the Cancer Center and the Department of Medicinal Chemistry, University of Minnesota, Minneapolis, Minnesota 55455 and Department of Chemistry, Rutgers University, Piscataway, New Jersey 08854

Received March 28, 2005; E-mail: trety001@umn.edu

Abstract: 1,2,3,4-Diepoxybutane (DEB) is a bifunctional electrophile capable of forming DNA−DNA and DNA−protein cross-links. DNA alkylation by DEB produces N7-(2′-hydroxy-3′,4′-epoxybut-1′-yl)-guanine monoadducts, which can then form 1,4-bis-(guan-7-yl)-2,3-butanediol (bis-N7G-BD) lesions. All three optical isomers of DEB are produced metabolically from 1,3-butadiene, but *S*,*S*-DEB is the most cytotoxic and genotoxic. In the present work, interstrand and intrastrand DNA−DNA cross-linking by individual DEB stereoisomers was investigated by PAGE, mass spectrometry, and stable isotope labeling. *S*,*S*-, *R*,*R*-, and *meso*-diepoxides were synthesized from L-dimethyl-2,3-*O*-isopropylidene-tartrate, D-dimethyl-2,3-*O*-isopropylidene-tartrate, and *meso*-erythritol, respectively. Total numbers of bis-N7G-BD lesions (intrastrand and interstrand) in calf thymus DNA treated separately with *S*,*S*-, *R*,*R*-, or *meso*-DEB (0.01−0.5 mM) were similar as determined by capillary HPLC−ESI$^+$-MS/MS of DNA hydrolysates. However, denaturing PAGE has revealed that *S*,*S*-DEB produced the highest number of interchain cross-links in 5′-GGC-3′/3′-CCG-5′ sequences. Intrastrand adduct formation by DEB was investigated by a novel methodology based on stable isotope labeling HPLC−ESI$^+$-MS/MS. *Meso* DEB treatment of DNA duplexes containing 5′-[1,7, NH_2-$^{15}N_3$,2-^{13}C-G]GC-3′/3′-CCG-5′ and 5′-GGC-3′/3′-CC[$^{15}N_3$,2-^{13}C-G]-5′ trinucleotides gave rise to comparable numbers of 1,2-intrastrand and 1,3-interstrand bis-N7G-BD cross-links, while *S*,*S* DEB produced few intrastrand lesions. *R*,*R*-DEB treated DNA contained mostly 1,3-interstrand bis-N7G-BD, along with smaller amounts of 1,2-interstrand and 1,2-intrastrand adducts. The effects of DEB stereochemistry on its ability to form DNA−DNA cross-links may be rationalized by the spatial relationships between the epoxy alcohol side chains in stereoisomeric N7-(2′-hydroxy-3′,4′-epoxybut-1′-yl)-guanine adducts and their DNA environment. Different cross-linking specificities of DEB stereoisomers provide a likely structural basis for their distinct biological activities.

Introduction

DNA−DNA cross-linking is recognized as the primary mechanism for the cytotoxic activity of many clinically useful antitumor drugs, including nitrogen mustards, chloroethylnitrosoureas, platinum agents, and mitomycin C[1]. Interchain DNA adducts prevent DNA strand separation, blocking DNA replication, transcription, and repair and leading to cancer cell death and the inhibition of tumor growth.[1,2] On the other hand, some nucleobase monoadducts and intrastrand DNA−DNA cross-links can be bypassed by DNA polymerases, potentially resulting in the insertion of incorrect nucleotides opposite the structurally altered base.[1,3−5] Despite their mutagenic side effects and, in some cases, the development of secondary malignancies associated with clinical application of DNA alkylating drugs,[6] they remain at the front lines of cancer therapy, prompting further investigations of their mechanisms with the goal of developing novel DNA targeting agents.[7−13]

S,*S*-1,2,3,4-Diepoxybutane (*S*,*S*-DEB) is a simple bis-epoxide cross-linking agent believed to be the active form of Ovastat (L-threitol-1,4-bismethanesulfonate) used clinically against ad-

[†] University of Minnesota.
[‡] Rutgers University.

(1) Rajski, S. R.; Williams, R. M. *Chem. Rev.* **1998**, *98*, 2723−2796.
(2) Skladanowski, A.; Konopa, J. *Biochem. Pharmacol.* **1994**, *47*, 2279−2287.
(3) Carmical, J. R.; Zhang, M.; Nechev, L.; Harris, C. M.; Harris, T. M.; Lloyd, R. S. *Chem. Res. Toxicol.* **2000**, *13*, 18−25.
(4) Carmical, J. R.; Kowalczyk, A.; Zou, Y.; Van Houten, B.; Nechev, L. V.; Harris, C. M.; Harris, T. M.; Lloyd, R. S. *J. Biol. Chem.* **2000**, *275*, 19482−19489.
(5) Kanuri, M.; Nechev, L. V.; Tamura, P. J.; Harris, C. M.; Harris, T. M.; Lloyd, R. S. *Chem. Res. Toxicol.* **2002**, *15*, 1572−1580.
(6) Sunters, A.; Grimaldi, K. A.; Souhami, R. L.; Hartley, J. A. *Nucleic Acids Res.* **1998**, *26*, 5617−5623.
(7) Sharma, S. K.; McLaughlin, L. W. *J. Am. Chem. Soc.* **2002**, *124*, 9658−9659.
(8) Noronha, A. M.; Wilds, C. J.; Miller, P. S. *Biochemistry* **2002**, *41*, 8605−8612.
(9) Wang, P.; Liu, R.; Wu, X.; Ma, H.; Cao, X.; Zhou, P.; Zhang, J.; Weng, X.; Zhang, X. L.; Qi, J.; Zhou, X.; Weng, L. *J. Am. Chem. Soc.* **2003**, *125*, 1116−1117.
(10) Richter, S. N.; Maggi, S.; Mels, S. C.; Palumbo, M.; Freccero, M. *J. Am. Chem. Soc.* **2004**, *126*, 13973−13979.
(11) Wilds, C. J.; Noronha, A. M.; Robidoux, S.; Miller, P. S. *J. Am. Chem. Soc.* **2004**, *126*, 9257−9265.
(12) Zhou, Q.; Duan, W.; Simmons, D.; Shayo, Y.; Raymond, M. A.; Dorr, R. T.; Hurley, L. H. *J. Am. Chem. Soc.* **2001**, *123*, 4865−4866.
(13) Mitra, K.; Marquis, J. C.; Hillier, S. M.; Rye, P. T.; Zayas, B.; Lee, A. S.; Essigmann, J. M.; Croy, R. G. *J. Am. Chem Soc.* **2002**, *124*, 1862−1863.

vanced ovarian cancer.[14−16] Ironically, *S*,*S*-DEB, along with *R*,*R*- and *meso*-DEB, is also the suspected carcinogenic metabolite of 1,3-butadiene (BD), a major industrial chemical used in the rubber and plastics industry and a recognized human carcinogen.[17,18] In vivo metabolic activation of BD to DEB is catalyzed by CYP2E1 and CYP2A6 monooxygenases. The first epoxidation step yields (*R*)- and (*S*)-3,4-epoxy-1-butene (EB).[19,20] EB can then be hydrolyzed to 1-butene-3,4-diol or can undergo the second oxidation to yield *R*,*R*-, *S*,*S*-, and *meso*-DEB.[21] Although DEB is a relatively minor metabolite of BD, available experimental evidence suggests that it is responsible for many of the adverse effects of BD. Biological studies indicate that DEB is 50−100-fold more genotoxic and mutagenic than its monoepoxide analogues, EB and 3,4-epoxy-1,2-butanediol,[22,23] likely a result of is ability to induce DNA−DNA and DNA-protein cross-links. Efficient metabolism of BD to DEB in target tissues of laboratory mice is thought to cause the extreme susceptibility of this species to BD carcinogenesis.[24]

The formation of DNA−DNA cross-links by DEB is a two-step process. Initial reactions of DEB with guanine nucleobases in DNA produce N7-(2′-hydroxy-3′,4′-epoxybut-1′-yl)-guanine (N7-HEBG) monoadducts, which can then be hydrolyzed to N7-(2′,3′,4′-trihydroxybut-1′-yl)-guanine (N7-THBG) or can alkylate neighboring nucleobases within the major groove of DNA to form bifunctional DNA adducts.[1,25] Although DNA−DNA cross-linking is less common than monoadduct formation, it is considered key for the ability of DEB to induce chromosomal aberrations, mutagenicity, cytotoxicity, and tumorigenic effects. Over 40 years ago, Lawley and Brookes first isolated guanine−guanine conjugates of DEB, which were identified as 1,4-bis-(guan-7-yl)-2,3-butanediol (bis-N7G-BD).[26] This structural assignment was recently confirmed in a series of detailed NMR experiments conducted in our laboratory.[27] Millard and collaborators used denaturing PAGE to demonstrate that, in analogy with nitrogen mustards, racemic DEB preferentially induces ***inter***strand DNA lesions at 5′-GNC sequences (N = G or C).[28,29] The formation of ***intra***strand cross-links by DEB has been hypothesized,[4] although no direct evidence for the presence of such lesions in DEB-treated DNA is available in the literature. Furthermore, the role of DEB stereochemistry in defining the efficiency and selectivity of DNA−DNA cross-linking has not been extensively explored.

The ability of DEB to display both antitumor and carcinogenic activity is of significant interest because of the widespread human exposure to BD in automobile exhaust and in tobacco smoke (20−75 μg per cigarette).[30] This dual activity may, at least in part, result from the presence of three distinct optical isomers of the diepoxide (*S*,*S*-, *R*,*R*-, and *meso*-DEB, Scheme 1).

Scheme 1. Structures of DEB Stereoisomers: *R*,*R*-DEB (**1a**), *S*,*S*-DEB (**1b**), and *meso*-DEB (**1c**)

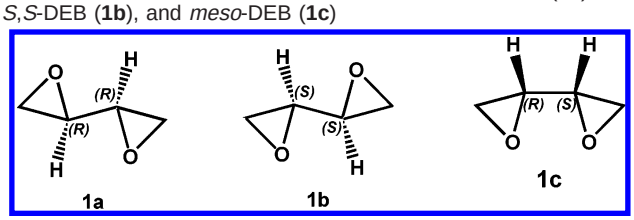

Biological studies reveal significant differences between the ability of DEB stereoisomers to inactivate T7 coliphage,[31] induce chromosomal aberrations,[32] and cause mutagenesis in maize.[33] Among the three stereoisomers, *S*,*S*-DEB exhibits the most potent genotoxicity and cytotoxicity, followed by *R*,*R*- and then *meso*-DEB.[31−33] Over 30 years ago, Feit and collaborators employed density gradient centrifugation to show that *meso*-DEB was less effective than *S*,*S*- and *R*,*R*-DEB in inducing interstrand DNA lesions.[31] This original investigation[31] suggested for the first time that the observed differences between the biological effects of DEB optical isomers may be structural in their origin.

In the present study, interstrand and intrastrand DNA−DNA cross-linking by individual DEB stereoisomers was directly investigated by a combination of mass spectrometry, gel electrophoresis, and a novel methodology based on stable isotope labeling of DNA. Our results provide evidence for stereospecific interactions between DEB stereoisomers and their DNA target, leading to differences in cross-linking specificity and, ultimately, in their biological activity.

Experimental Section

Note: DEB is a suspected human carcinogen and must be handled with adequate safety precautions.

Materials and General Methods. Dimethyl 2,3-*O*-isopropylidene-L-tartrate, dimethyl 2,3-*O*-isopropylidene-D-tartrate, racemic DEB, *meso*-erythritol, lithium aluminum hydride, methansulfonyl chloride, pyridine, and methansulfonic acid were purchased from Sigma-Aldrich (Milwaukee, WI, St. Louis, MO). $CDCl_3$ was obtained from Cambridge Isotope Laboratories (Andover, MA). Racemic bis-N7G-BD, N7-THBG, and $^{15}N_5$-N7-THBG were prepared as described previously.[27] High-resolution mass spectra were obtained on a Bruker BioTOF II. UV spectra were recorded with a Beckman DU 7400 spectrophotometer. Proton NMR spectra were obtained on a 600 MHz Varian Inova NMR spectrometer.

Gas chromatography−positive ion chemical ionization mass spectrometry (GC−MS) experiments were carried out on an HP5890 series II gas chromatograph (Agilent Technologies, Palo Alto, CA). The GC was fitted with a 30 m × 0.25 mm × 0.25 μm film thickness DB-17MS column (Agilent Technologies) and a 2 m × 530 μm uncoated deactivated fused silica precolumn. Helium was used as a carrier gas with a constant flow of 0.7 mL/min. A 1 μL volume of each sample was injected via splitless injection with a gooseneck splitless liner. The splitless vent flow was 50 mL/min, the purge open time was 0.5 min, and the injector temperature was 200 °C. GC oven temperature was

(14) Schmidmaier, R.; Oellerich, M.; Baumgart, J.; Emmerich, B.; Meinhardt, G. *Exp. Hematol.* **2004**, *32*, 76−86.
(15) Hartley, J. A.; O'Hare, C. C.; Baumgart, J. *Br. J. Cancer* **1999**, *79*, 264−266.
(16) Runowicz, C. D.; Fields, A. L.; Goldberg, G. L. *Cancer* **1995**, *76*, 2028−2033.
(17) Melnick, R. L.; Kohn, M. C. *Carcinogenesis* **1995**, *16*, 157−163.
(18) Rice, J. M.; Boffetta, P. *Chem. Biol. Interact.* **2001**, *135*−*136*, 11−26.
(19) Malvoisin, E.; Roberfroid, M. *Xenobiotica* **1982**, *12*, 137−144.
(20) Himmelstein, M. W.; Turner, M. J.; Asgharian, B.; Bond, J. A. *Toxicology* **1996**, *113*, 306−309.
(21) Krause, R. J.; Elfarra, A. A. *Arch. Biochem. Biophys.* **1997**, *337*, 176−184.
(22) Sasiadek, M.; Norppa, H.; Sorsa, M. *Mutat. Res.* **1991**, *261*, 117−121.
(23) Cochrane, J. E.; Skopek, T. R. *Carcinogenesis* **1994**, *15*, 713−717.
(24) Henderson, R. F.; Thornton-Manning, J. R.; Bechtold, W. E.; Dahl, A. R. *Toxicology* **1996**, *113*, 17−22.
(25) Lawley, P. D.; Brookes, P. *Nature* **1965**, *206*, 480−483.
(26) Lawley, P. D.; Brookes, P. *J. Mol. Biol.* **1967**, *25*, 143−160.
(27) Park, S.; Tretyakova, N. *Chem. Res. Toxicol.* **2004**, *17*, 129−136.
(28) Millard, J. T.; White, M. M. *Biochemistry* **1993**, *32*, 2120−2124.
(29) Sawyer, G. A.; Frederick, E. D.; Millard, J. T. *Chem. Res. Toxicol.* **2004**, *17*, 1057−1063.
(30) Hecht, S. S. *J. Natl. Cancer Inst.* **1999**, *91*, 1194−1210.
(31) Verly, W. G.; Brakier, L.; Feit, P. W. *Biochim. Biophys. Acta* **1971**, *228*, 400−406.
(32) Matagne, R. *Mutat. Res.* **1969**, *7*, 241−247.
(33) Bianchi, A.; Contin, M. *J. Heredity* **1962**, *53*, 277−281.

held at 40 °C for 2 min and then ramped at 3 °C/min until 80 °C. The CI source parameters were as follows: filament emission current, 178 μA; electron energy, 193 eV; ion source temperature, 250 °C. A mixture of NH_3 (4%) and CH_4 (96%) was used as the reagent gas. For all samples analyzed, *m*/*z* 104 $[M + NH_4]^+$ was monitored. The peak width was 0.8 amu, and the scan time was 0.2 s.

***S,S*- and *R,R*-1,2,3,4-Diepoxybutane.** Optically active *S,S*- and *R,R*-DEB stereoisomers were prepared as described in the literature[34−36] starting with dimethyl 2,3-*O*-isopropylidene-L-tartrate and dimethyl 2,3-*O*-isopropylidene-D-tartrate, respectively.

S,S-1,2,3,4-Diepoxybutane: clear oil, bp 138−140 °C; ^{1}H NMR ($CDCl_3$) δ (ppm) 2.70−2.72 (2H, m), 2.80−2.82 (2H, m), 2.86−2.88 (2H, m); ^{13}C ($CDCl_3$) δ (ppm) 51.4, 43.6.

R,R-1,2,3,4-Diepoxybutane: clear oil, bp 138−140 °C;^{1}H NMR-($CDCl_3$) δ (ppm) 2.70−2.72 (2H, m), 2.79−2.81 (2H, m), 2.86−2.88 (2H, m); ^{13}C ($CDCl_3$) δ (ppm) 51.5, 43.6.

***meso*-1,2,3,4-Diepoxybutane.** *meso*-1,2,3,4-Diepoxybutane was prepared from *meso*-erythritol according to the published procedure.[37] Clear oil, bp 138−140 °C; ^{1}H NMR ($CDCl_3$) δ (ppm) 2.65−2.72 (2H, m), 2.75−2.82 (2H, m), 2.91−2.95 (2H, m). ^{13}C ($CDCl_3$) δ (ppm) 50.3, 44.2. The diastereomeric purity as determined by NMR and GC−MS signal integration was ∼95%.

***meso*-1,4-Bis-(guan-7-yl)-2,3-butanediol.** Guanosine (1.00 g, 3.53 mmol) was suspended in 20 mL of glacial acetic acid and stirred at 80 °C for 1 h. *meso*-DEB (300 μL, 3.88 mmol) was added to initiate the reaction, and the mixture was stirred at 80 °C for 4 h. Once cooled to room temperature, 100 mL of acetone/diethyl ether (1:4) were slowly added over the course of 30 min under vigorous stirring. The resulting light yellow solid containing the bifunctional lesion was filtered, rinsed with diethyl ether, and dried under nitrogen. To remove the ribosyl groups, the precipitate was resuspended in 25 mL of 1 N HCl solution and stirred at 85 °C for 1 h. The mixture was cooled to room temperature, and the solvent was evaporated, affording a white solid. *meso*-Bis-N7G-BD was recrystallized from 1 N NaOH to give 37.8 mg of the product (5.5% yield). Chemical and diastereoisomeric purity of the product (>95%) was established by HPLC, NMR spectroscopy, and mass spectrometry. Standard solution concentrations were determined by UV spectrophotometry (ϵ_{252} = 15,700 at pH 1).[27]

Racemic and *meso*-$^{15}N_{10}$-1,4-Bis-(guan-7-yl)-2,3-butanediol. $^{15}N_5$-dGTP (3.3 mg, from Martek Biosciences, Columbia, MD) was dissolved in 100 μL of glacial acetic acid. A 0.5 μL aliquot of either racemic or *meso*-DEB was added, followed by incubation at 80 °C for 2 h. The reaction mixture was cooled to room temperature, and ethyl acetate was added to cause precipitate formation. The resulting solid was removed, washed with ethyl acetate, and redissolved in 300 μL of 1 N HCl. Hydrolysis was performed at 80 °C for 1 h to achieve depurination. The solution was dried under reduced pressure, and the residue was dissolved in 1 mL of water and purified by SPE using Waters SepPak C18 cartridges. Standard solution concentrations were established by HPLC−ESI$^+$-MS/MS and HPLC−UV peak integration in comparison with unlabeled bis-N7G-BD diastereomers.

DEB Treatment of Calf Thymus DNA and Cross-Link Analyses. Calf thymus DNA (CT DNA, 1 mg/mL solution in 10 mM Tris-HCl buffer, pH 7.2, in triplicate) was treated with *R,R*-, *S,S*-, or *meso*-DEB (0.01−0.5 mM) at 37 °C for 24 h. The unreacted DEB was extracted with diethyl ether (2 × 400 μL). Samples were spiked with known amounts of racemic and *meso*-$^{15}N_{10}$-bis-N7G-BD (15−20 pmol) and subjected to either neutral thermal or acid hydrolysis. Neutral thermal hydrolysis was performed at 80 °C for 1 h, while acid hydrolysis was achieved by heating in 0.1 N HCl (80 °C for 1 h). Partially depurinated DNA backbone was removed by ultrafiltration through Microcon YM-30 membrane filters (Millipore - Bedford, MA), and the filtrates were directly analyzed by HPLC−ESI$^+$-MS/MS as described below.

Detection of Interstrand DEB Cross-Links by Denaturing PAGE. Synthetic DNA 28-mers (5′-TAT ATA TTT ATA GGC TAT TAT TAT ATT A) (+ strand), (5′-TAA TAT AAT AAT AGC CTA TAA ATA TAT A) (− strand) were prepared by standard phosphoramidite chemistry. Both strands were purified by 20% denaturing PAGE.[38] The (+) strand (200 pmol) was 5′-endlabeled with ^{32}P in the presence of [γ-^{32}P]ATP/T4 polynucleotide kinase[38] and then spiked with the corresponding unlabeled DNA (20 nmol). The DNA was annealed to the complementary (−) strand (22 nmol), and the resulting double stranded DNA was dissolved in 0.3 mM NaOAc, pH 5.0, and treated with 0, 10, 50, or 100 mM of *R,R*-, *S,S*-, racemic, or *meso*-DEB for 3 h at 37 °C. The DNA solution was dried under vacuum, and the residue was dissolved in a 1:1 mixture of water and formamide (5 μL). The solution was loaded onto 20% denaturing PAGE (0.4 mm, 41 cm × 37 cm), run at 60 W and at ambient temperature. Radiolabeled DNA bands were visualized with a Storm 840 phosphorimager. The cross-linked products were detected as low-mobility bands on the gel, and their identity was confirmed by capillary HPLC−ESI$^-$-MS/MS analysis of the material eluted from the gel (M = 17 254 (calculated), M = 17 254 (observed)). The bands were quantified by volume analysis, and cross-linking efficiency was quantified from the intensity ratio of the cross-linked band versus the band corresponding to single-stranded DNA.

Capillary HPLC−ESI$^-$-MS/MS analysis of cross-linked DNA was performed on an 1100 Agilent Technologies capillary HPLC−MSD ion trap system operated in the negative ion mode. A Zorbax Extend-C18 column (0.5 mm × 150 mm, 3.5 μm, Agilent Technologies) was eluted at a flow rate of 12 μL/min, with a linear gradient of 15 mM ammonium acetate (A) and acetonitrile (B). The mobile phase composition was kept at 1% B for 5 min, then increased to 25% B for 15 min, and further to 25% B at 30 min. The mass range was *m*/*z* 500−1900, and the target ion abundance was 30 000. ESI was achieved with a spray voltage of +2.6 kV and a source temperature of 200 °C. The nebulizing gas (N_2) pressure was set to 15 psi, and the drying gas (N_2) flow rate was set to 5 L/min.

Stable Isotope Labeling to Quantify Intrastrand and Interstrand Bis-N7G-BD Cross-Links in 5′-GGC Context. The DNA 28-mer (5′-TAT ATA TTT ATA GGC TAT TAT TAT ATT A) (+ strand) and the complementary strand (5′-TAA TAT AAT AAT A[1,7,NH_2-$^{15}N_3$-2-^{13}C-G]C CTA TAA ATA TAT A) were synthesized by standard phosphoramidite methodology. 1,7,NH_2-$^{15}N_3$-2-^{13}C-dG phosphoramidite was prepared at Rutgers University as previously described.[39] Both oligodeoxynucleotides were purified by HPLC with an Agilent Technologies HPLC system (model 1100) incorporating a UV diode array detector and a semi-micro UV cell. A Supelcosil LC-18-DB column (4.6 × 150 mm, 5 μm) was eluted at a flow rate of 1 mL/min with a gradient of 150 mM ammonium acetate (A) and acetonitrile (B). Solvent composition was changed from 5 to 15% B in 40 min. HPLC fractions corresponding to full-length oligodeoxynucleotide products were collected, combined, and dried under vacuum. DNA purity and identity were determined by HPLC−ESI$^-$ MS (+ strand: calcd M = 8580.7, obsd M = 8581.2; − strand: calcd M = 8588.7, obsd M = 8589.5).

To obtain double-stranded DNA, (+) strand (20 nmol) and (−) strand (22 nmol) were combined, dried under vacuum, and dissolved in 180 μL of 0.3 mM sodium acetate buffer, pH 5.0 containing 0.1 mM Tris, and 0.5 mM NaCl. 10% excess of the (−) strand was used to ensure that the (+) strand remained double-stranded throughout the duration of the experiment (calculated T_m = 43 °C). The solution was heated to 90 °C and allowed to slowly cool to room temperature to form double-

(34) Feit, P. W. *J. Med. Chem.* **1964**, *7*, 14−17.
(35) Mash, E. A.; Nelson, K. A.; Van Deusen, S.; Hemperly, S. B. *Org. Synth.* **1990**, *68*, 92−103.
(36) Robbins, M. A.; Devine, P. N.; Oh, T. *Org. Synth.* **1999**, *76*, 101−109.
(37) Claffey, D. J. *Synth. Commun.* **2002**, *32*, 3041−3045.
(38) Sambrook, J.; Fritsch, E. F.; Maniatis, T. *Molecular Cloning: A Laboratory Manual*; Cold Spring Harbor Press: 1989.
(39) Shallop, A. J.; Gaffney, B. L.; Jones, R. A. *J. Org. Chem.* **2003**, *68*, 8657−8661.

stranded DNA. The DNA (1.5 nmol, 15 μL aliquots) was treated with *R,R*-, *S,S*-, racemic, or *meso*-DEB (10 equiv) for 3 h at 25 °C and precipitated with cold ethanol. The reaction mixtures were resuspended in water, spiked with 1.5 pmol of racemic and *meso*-$^{15}N_{10}$-1,4-bis-N7G-BD (internal standard for HPLC−ESI$^+$-MS/MS), and subjected to thermal or acid hydrolysis as described above. The hydrolysates were directly analyzed by HPLC−ESI$^+$-MS/MS. The relative contribution of intrastrand and interstrand cross-linking was determined from the HPLC−MS/MS peak areas corresponding to bis-N7G-BD (*m/z* 389.2 $[M + H]^+ \rightarrow$ 152.1 $[Gua + H]^+$) and [$^{15}N_3$, $^{13}C_1$]-bis-N7G-BD (393.2 $[M + H]^+ \rightarrow$ 156.0 [$^{15}N_3$,$^{13}C_1$-Gua + H]$^+$, 152.1 $[Gua + H]^+$), respectively.

Stable Isotope Labeling To Determine the Kinetics of Spontaneous Hydrolysis of Intrastrand and Interstrand Bis-N7G-BD in Double-Stranded DNA. The DNA 28-mer (5′-TAT ATA TTT ATA GGC TAT TAT TAT ATT A) (+ strand) and the complementary strand (5′-TAA TAT AAT AAT A[1,7,NH$_2$-$^{15}N_3$-2-^{13}C-G]C CTA TAA ATA TAT A) were prepared and annealed as described above. The $^{15}N_3$-2-^{13}C-labeled duplex (15 nmol) was dissolved in 240 μL of 0.3 mM NaOAc, pH 5.0 and treated with *R,R*-DEB (10 μL) for 3 h at 37 °C to generate both interstrand and intrastrand bis-N7G-BD adducts. The DNA was precipitated with cold ethanol, dried under nitrogen, and redissolved in 125 μL of 10 mM Tris buffer containing 0.2 N NaCl. Following the addition of $^{15}N_{10}$-1,4-bis-N7G-BD internal standard (25 pmol), the solution was maintained at 37 °C. Aliquots (20 μL) were removed following incubation for 0, 1, 3, 6, 9, 16, and 20 h and immediately frozen at −20 °C. The hydrolysates were directly analyzed by HPLC−ESI$^+$-MS/MS as described below. The autosampler tray was maintained at 4 °C to minimize further depurination. The amounts of hydrolytically released intrastrand and interstrand bis-N7G-BD cross-links were determined from HPLC−ESI$^+$-MS/MS peak areas corresponding to bis-N7G-BD (*m/z* 389.2→ 238.0) and [$^{15}N_3$]-bis-N7G-BD (*m/z* 393.2 → 238.0; 242.0), respectively. $^{15}N_{10}$-Bis-N7G-BD internal standard was detected analogously by monitoring the transition *m/z* 399.2 → 243.0. To determine the total number of bis-N7G-BD adducts in this DNA, several aliquots were analyzed following quantitative release of the cross-links by thermal hydrolysis (70 °C for 1 h). First-order constants (k) were calculated from the slope of the plot of $\ln[c/c_0] = -kt$, where t is the incubation time, c is the concentration of bis-N7G-BD remaining in DNA at the time t, and c_0 is the starting concentration of bis-N7G-BD in DNA.

Stable Isotope Labeling Experiments to Distinguish between 1,2 (GC) and 1,3 (GNC) Interstrand Cross-Linking by DEB. DNA 28-mer (5′-TAT ATA TTT ATA [1,7,NH$_2$-$^{15}N_3$-2-^{13}C−G] GC TAT TAT TAT ATT A) (+ strand) and its unlabeled complement were prepared as described above. Double-stranded DNA (7 nmol) was treated with *S,S*-, *R,R*-, racemic, or *meso*-DEB (50 mM) in 0.3 mM sodium acetate buffer (pH 5, total volume = 72 μL). The reaction mixture was incubated at 37 °C for 3 h, dried under vacuum, and separated by 20% denaturing PAGE (2,000 V, for 2.5 h). The position of the slowly migrating band containing [1,7,NH$_2$-$^{15}N_3$-2-^{13}C]-labeled interstrand DNA cross-links was estimated based on the analogous band from the unlabeled DNA reaction (20 nmol duplex, treated with a 100× molar excess of *S,S*-DEB), which was visualized by UV shadowing. The DNA bands containing interstrand DEB cross-links were excised, and the DNA was extracted by standard "crash and soak" methods (10 mM Tris-Cl, 1 mM EDTA, pH 7.6; overnight).[38] The DNA was desalted by SPE on Waters C_{18} SepPak cartridges eluted with methanol/water, dried, and dissolved in 15 μL of water. DEB-induced N7-guanine cross-links were released by thermal or acid hydrolysis as described above. The molar ratio of 1,3-interstrand and 1,2-interstrand G−G DEB cross-links was established from the HPLC−ESI$^+$-MS/MS peak area ratio corresponding to [1,7,NH$_2$-$^{15}N_3$-2-^{13}C]-labeled and unlabeled bis-N7G-BD, respectively.

Capillary HPLC−ESI$^+$-MS/MS. An Agilent 1100 capillary HPLC system (Wilmington, DE) interfaced to a Finnigan TSQ Quantum triple quadrupole mass spectrometer was used in all analyses. Chromatographic separation was achieved with a Zorbax SB-C18 column (150 mm × 0.5 mm, 5 μm) eluted with 15 mM ammonium acetate, pH 5.5 (A) and acetonitrile (B). A linear gradient was from 0 to 10% B in 20 min at a flow rate of 10 μL/min, and the injection volume was 8 μL. To minimize salt contamination, HPLC effluent from the first 3 min of each run was diverted to waste. The mass spectrometer was operated in the positive ion mode with nitrogen as a sheath gas (5 L/min). Electrospray ionization was achieved at a spray voltage of 4.0 kV, and the capillary temperature was 250 °C. Bis-N7G-BD cross-links were detected in selected reaction monitoring mode as described below.

Bis-N7G-BD lesions formed in DEB-treated calf thymus DNA were quantified by isotope dilution with racemic and *meso*-$^{15}N_{10}$-bis-N7G-BD internal standards. Quantitative analyses were performed using HPLC−ESI$^+$ MS/MS peak areas corresponding to bis-N7G-BD (*m/z* 389.2 $[M + H]^+ \rightarrow$ 238.0 $[M + H\text{-Gua}]^+$, 389.2 → 220.0 $[M + H\text{-Gua} - H_2O]^+$). Internal standards *meso*- and racemic $^{15}N_{10}$-bis-N7G-BD were analyzed analogously using the transitions *m/z* 399.2 $[M + H]^+ \rightarrow$ 243.0 $[M + H\text{-}^{15}N_5\text{-Gua}]^+$, 399.2 → 225.0 $[M + H\text{-}^{15}N_5\text{-Gua} - H_2O]^+$. Quantitation of N7-THBG was achieved using the reconstructed ion chromatograms corresponding to the MS/MS transition: *m/z* = 256.0 $[M + H]^+ \rightarrow$ 152.0 $[M + H\text{-THB}]^+$ and the corresponding transition *m/z* = 261.0 $[M + H]^+ \rightarrow$ 157.0 $[M + H\text{-THB}]^+$ of the $^{15}N_5$-THBG internal standard.[40−42] Calibration curves were constructed by analyzing standard solutions containing known amounts of each adduct and its internal standard, followed by regression analysis of the HPLC−ESI$^+$-MS/MS peak area ratios.

Intrastrand and interstrand bis-N7G-BD cross-links originating from $^{15}N_3$,$^{13}C_1$-dG containing 28-mer (5′-TAT ATA TTT ATA GGC TAT TAT TAT ATT A) (+ strand), (5′-TAA TAT AAT AAT A[1,7,NH$_2$-$^{15}N_3$-2-^{13}C−G]C CTA TAA ATA TAT A) (− strand) were quantified using the transitions *m/z* = 389.2 $[M + H]^+ \rightarrow$ 152.0 $[Gua + H]^+$ (intrastrand) and 393.2 $[M + H]^+ \rightarrow$ 156.0 [$^{15}N_3{}^{13}C_1$-Gua + H]$^+$, 152.0 $[Gua + H]^+$ (interstrand). The molar ratios between interstrand and intrastrand bis-N7G-BD lesions were determined directly from the corresponding HPLC−ESI$^+$-MS/MS peak areas.

1,2-/1,3-Interstrand bis-N7G-BD cross-links originating from [1,7,-NH$_2$-$^{15}N_3$-2-^{13}C]- dG containing 28-mer (5′-TAT ATA TTT ATA [1,7,-NH$_2$-$^{15}N_3$-2-^{13}C-G] GC TAT TAT TAT ATT A) (+ strand), 5′-TAA TAT AAT AAT AG CTA TAA ATA TAT A) (− strand) were quantified following thermal or acid hydrolysis of interstrand DNA−DNA cross-links isolated by denaturing PAGE. HPLC−ESI$^+$-MS/MS settings were as described in the preceding section. MS/MS transitions *m/z* 389.2 $[M + H]^+ \rightarrow$ 152.0 $[Gua + H]^+$ and *m/z* 393.2 $[M + H]^+ \rightarrow$ 155.0 [$^{15}N_3{}^{13}C_1$-Gua + H]$^+$, 152.0 $[Gua + H]^+$ were used to quantify 1,3- and 1,2-interstrand bis-N7G-BD lesions, respectively.

Results

DEB stereoisomers induce similar numbers of bis-N7G-BD adducts. Bifunctional alkylation of DNA by DEB gives rise to 1,4-bis-(guan-7-yl)-2,3-butanediol (bis-N7G-BD) adducts (**2**−**4** in Scheme 2).[27] Because N-7 alkylation of guanine in DNA generates a quaternized nitrogen, destabilizing the glycosidic bond, these lesions are hydrolytically labile and can be selectively released from the DNA backbone as free bases upon heating at neutral pH. We have previously analyzed the formation of racemic bis-N7G-BD lesions in D,L-DEB-treated DNA by HPLC−ESI$^+$-MS/MS analysis of thermal DNA hydrolysates.[27] Bis-N7G-BD and the corresponding N7-(2′,3′,4′-

(40) Tretyakova, N. Y.; Chiang, S. Y.; Walker, V. E.; Swenberg, J. A. *J Mass Spectrom.* **1998**, *33*, 363−376.
(41) Koc, H.; Tretyakova, N. Y.; Walker, V. E.; Henderson, R. F.; Swenberg, J. A. *Chem. Res. Toxicol.* **1999**, *12*, 566−574.
(42) Oe, T.; Kambouris, S. J.; Walker, V. E.; Meng, Q.; Recio, L.; Wherli, S.; Chaudhary, A. K.; Blair, I. A. *Chem. Res. Toxicol.* **1999**, *12*, 247−257.

Scheme 2. Structures of Stereoisomeric 1,4-bis-(guan-7-yl)-2,3-butanediol (bis-N7G-BD) Adducts

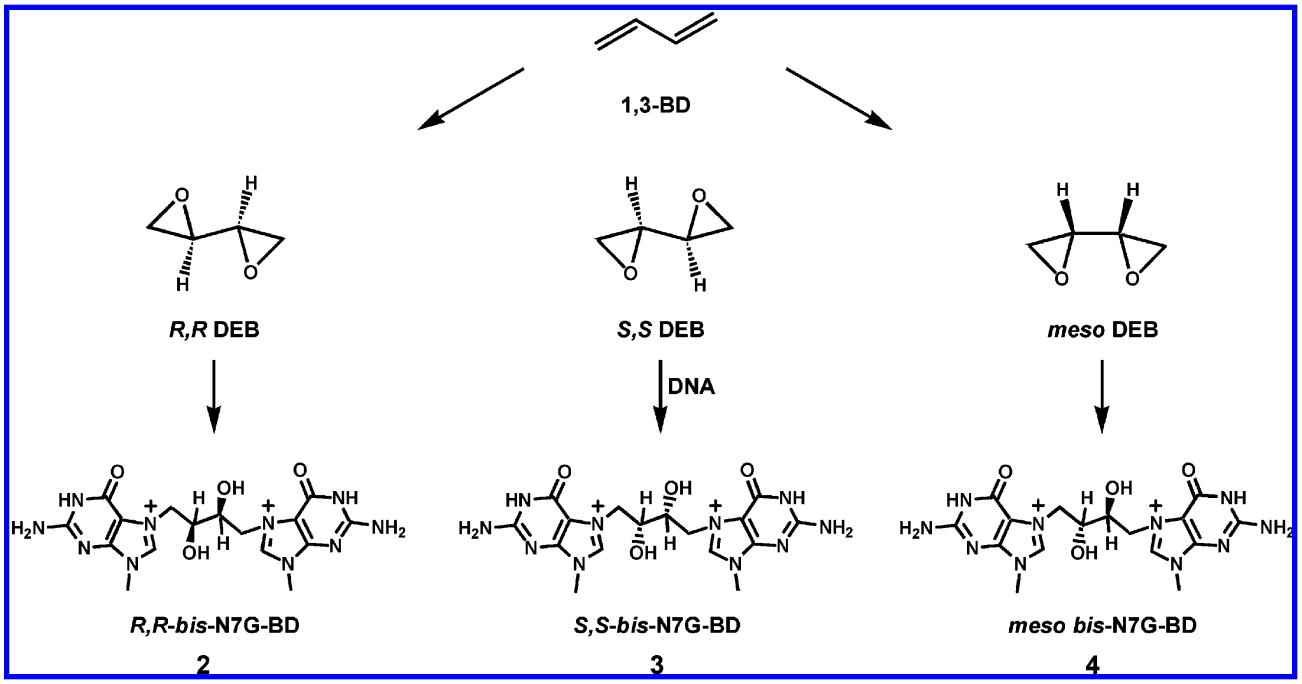

trihydroxybut-1′-yl)guanine (N7-THBG) monoadducts were formed in a concentration-dependent fashion, with similar amounts of N7−N7-G cross-links and monoadducts produced at low exposure concentrations (0.05−0.1 mM DEB) and N7-THBG predominating at higher DEB exposures.[27]

In the present work, the formation of diastereomeric bis-N7G-BD lesions **2**−**4** in double-stranded DNA treated with individual DEB stereoisomers was investigated in order to compare their ability to induce bifunctional DNA adducts. G−G DEB conjugates were quantified as free bases following their release from the DNA backbone,[27] thus providing the total amounts of guanine−guanine butanediol cross-links generated by *S*,*S*-, *R*,*R*-, and *meso*-DEB, irrespective of their type (interstrand or intrastrand). Low DEB concentrations (0.01−0.5 mM) were employed to maximize cross-linking selectivity and to mimic physiological exposures. Accurate and specific quantification of stereoisomeric bis-N7G-BD adducts was achieved by isotope dilution capillary HPLC−ESI$^+$-MS/MS using synthetic racemic and *meso*-$^{15}N_{10}$-bis-N7G-BD internal standards.[27] While the two optically active bis-N7G-BD lesions (**2** and **3** in Scheme 2) are enantiomeric and thus have identical HPLC retention times, the *meso* cross-link (**4** in Scheme 2) elutes slightly later from the HPLC column (see Supporting Information).

Bis-N7G-BD amounts increased in a dose-dependent manner in double-stranded DNA (calf thymus DNA) treated with 0.01−0.5 mM *S*,*S*-, *R*,*R*-, or *meso*-DEB (Figure 1). Adduct quantities ranged between 0.001 and 0.3 per 10^3 normal guanines, depending on exposure concentration (Figure 1). However, the number of cross-linked lesions was only moderately affected by diepoxide stereochemistry (Figure 1). Similarly, the amounts of N7-THBG monoadducts in these DNA samples were comparable, regardless of the DEB isomer used (results not shown). Taken together, these results rule out stereospecific differences between the total reactivity of DEB isomers toward double-stranded DNA.

S,S-DEB is the most efficient interstrand DNA-DNA cross-linker. We next examined the ability of *S*,*S*-, *R*,*R*-, and *meso*-DEB to induce interstrand DNA−DNA cross-links. ^{32}P end-labeled DNA duplexes containing a complementary 5′-GGC-3′/3′-CCG-5′ trinucleotide flanked by AT-rich regions (5′-TAT ATA TTT ATA GGC TAT TAT TAT ATT A) (+ strand), (5′-TAA TAT AAT AAT AGC CTA TAA ATA TAT A) (− strand) were incubated with individual DEB stereoisomers. 5′-GGC-3′ sequences have been previously identified as the target sites for DEB-induced interstrand DNA cross-linking.[28,29] Denaturing PAGE of DEB-treated duplexes has revealed the formation of interchain linkages as indicated by the appearance of a new DNA band with approximately half the mobility of the corresponding single strands (Figure 2). ESI$^-$-MS analysis of this material following extraction from the gel confirmed that it represented cross-linked duplexes containing a single butanediol linkage (calculated M = 17 254; observed M = 17 254, Figure 3). For each DEB stereoisomer, the cross-linked band increased in intensity as the DEB concentration was raised from 10 to 50 mM and further to 100 mM (Figure 2). Furthermore, interstrand cross-linking efficiency

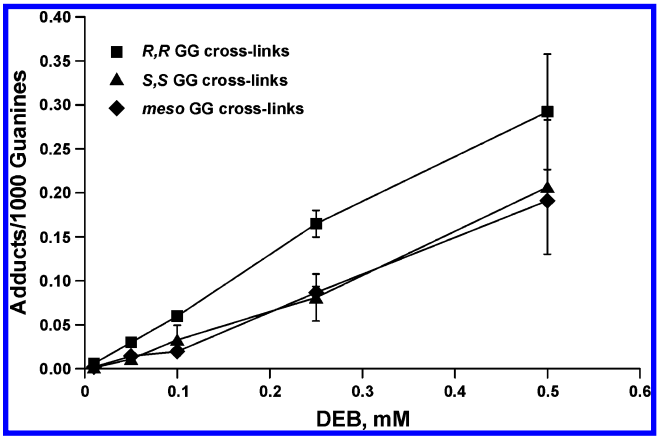

Figure 1. Formation of 1,4-bis-(guan-7-yl)-2,3-butanediol lesions in calf thymus DNA treated with individual stereoisomers of DEB (0.01−0.5 mM). Bis-N7G-BD adduct amounts (intrastrand + interstrand) were determined by capillary HPLC−ESI$^+$-MS/MS analysis of DNA hydrolysates.

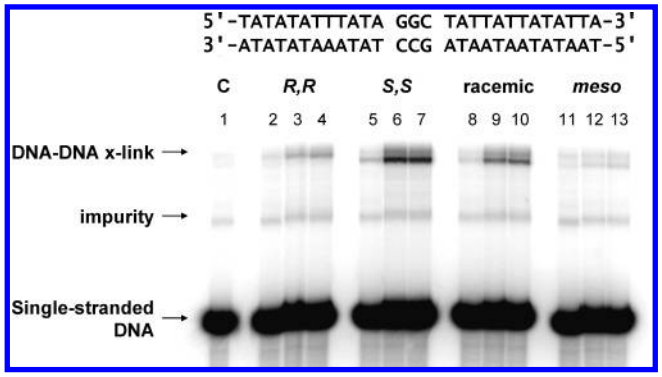

Figure 2. 20% Denaturing PAGE of synthetic DNA duplexes (5′-TAT ATA TTT ATA *GGC* TAT TAT TAT ATT A, (+) strand) following their incubation with *R,R*- (lanes 2−4), *S,S*- (lanes 5−6), racemic (lanes 8−10), and *meso*-DEB (lanes 11−13). DEB concentrations were as follows: 0 mM (lane 1, control DNA); 10 mM (lanes 2, 5, 8, and 11); 50 mM (lanes 3, 6, 9, and 12); and 100 mM (lanes 4, 7, 10, 13). Interstrand cross-links (x-links) are observed as slowly moving bands on the gel.

differed significantly for *S,S*, *R,R*, and *meso* isomers of DEB (Figure 2). The number of interstrand cross-links was the highest for *S,S*-DEB, followed by racemic, *R,R*-, and *meso*-diepoxide (Figure 2). Quantitative densitometry analysis indicated that, at the highest exposure level (100 mM), *S,S*-DEB induced 8-fold and 10-fold more interstrand lesions than did *R,R*- and *meso*-diepoxides, respectively. These results demonstrate that *S,S*-DEB is a more effective interstrand DNA−DNA cross-linker than *R,R*- and *meso*-DEB, consistent with its potent cytotoxicity.[31,32]

meso*-DEB produces 1,2-intrastrand N7G−N7G cross-links.** Our observation of similar total numbers of bis-N7G-BD cross-links in DNA treated with different DEB stereoisomers (Figure 1), but a greater ability of *S,S*-DEB to induce ***interstrand DNA cross-links (Figure 2), can potentially be explained by the formation of ***intra***strand bis-N7G-BD lesions by *meso*- and *R,R*-DEB, but not *S,S*-DEB. Unfortunately, such intrastrand DNA cross-linking cannot be analyzed by standard methods. Denaturing PAGE[43] cannot directly detect intrastrand lesions because their gel mobility is similar to that of the corresponding single strands. Mass spectrometry analysis of nuclease digests[44,45] is not readily applicable to N7-guanine lesions because of their hydrolytic lability, which leads to inadvertent depurination during enzymatic digestion.

We developed a novel strategy based on stable isotope labeling−mass spectrometry methodology (Figure 4) to separately quantify intrastrand and interstrand bis-N7G-BD cross-links in DEB-treated DNA. A DNA duplex containing a single 5′-GGC-3′ trinucleotide flanked by two AT-rich sequences was prepared. Only native bases were incorporated into the (+) strand, while the (−) strand contained a single [$^{15}N_3$,$^{13}C_1$]-guanine opposite GGC (Figure 4):

5'-GG C - 3'
3'-CC[$^{15}N_3$,$^{13}C_1$-G] – 5'

Since the only guanine present in the (−) strand has the $^{15}N_3$,$^{13}C_1$ isotope tag, any interstrand G−G conjugates originating from this duplex must possess the $^{15}N_3$,$^{13}C_1$ label, with a corresponding (+4) mass shift detectable by mass spectrometry (Figure 4). In contrast, intrastrand G−G DEB lesions originate exclusively from the unlabeled (+) strand and thus will not contain the $^{15}N_3$,$^{13}C_1$ label (Figure 4). HPLC−ESI$^+$-MS/MS analysis of DNA hydrolysates can readily distinguish between [$^{15}N_3$,$^{13}C_1$]-labeled and unlabeled bis-N7G-BD conjugates (*m/z* 393.2 and 389.2 $(M + H)^+$, respectively) and thus can determine the relative extent of intrastrand and interstrand cross-linking by DEB. A 10% molar excess of the (−) strand was employed to ensure that the (+) strand remained hybridized to its complement throughout the duration of the experiment.

The [$^{15}N_3$,$^{13}C_1$]-labeled duplex was treated with *S,S*-, *R,R*-, racemic, or *meso*-DEB (10 molar equiv), followed by HPLC−ESI$^+$-MS/MS analyses of bis-N7G-BD and [$^{15}N_3$,$^{13}C_1$]-bis-N7G-BD in DNA hydrolysates. Extracted ion chromatograms corresponding to unlabeled G−G DEB cross-links (Figure 5A) contain a prominent peak with HPLC retention time and MS/MS fragmentation pattern identical to those of synthetic bis-N7G-BD (*m/z* 389.2 → 238.0 $(M + H\text{-Gua})^+$, 220 $(M + H\text{-Gua} - H_2O)^+$, and 152 $(Gua + H)^+$, see Figure 5A, insert).[27] The corresponding [$^{15}N_3$,$^{13}C_1$]-labeled lesions are observed at *m/z* 393.2 (Figure 5B), exhibiting two series of ions consistent with the presence of both guanine and $^{15}N_3$,$^{13}C_1$-guanine in the molecule: *m/z* 393.2 $[M + H]^+$→ *m/z* 242.0 $(M + H\text{-Gua})^+$, 238.0 $(M + H\text{-}[^{15}N_3, ^{13}C_1]\text{-Gua})^+$, 224.0 $(M + H\text{-Gua} - H_2O)^+$, 220.0 $(M + H\text{-}[^{15}N_3,^{13}C_1]\text{Gua} - H_2O)^+$, 156.0 $([^{15}N_3, ^{13}C_1]\text{-Gua} + H)^+$, and 152.0 $(Gua + H)^+$ (Figure 5B, inset).

The formation of unlabeled bis-N7G-BD (*M* = 388.2, *m/z* 389.2 $[M + H]^+$) following *meso*-DEB treatment of the 5′-GGC-3′/3′-CC[$^{15}N_3$,$^{13}C_1$]G-5′ duplex (Figure 5A) provides the first direct evidence for the formation of intrastrand DNA lesions by DEB. Similar results were obtained when bis-N7G-BD adducts were released by acid hydrolysis (0.1 N HCl, 1 h at 70 °C), ruling out the possibility of artifactual bis-N7G-BD formation by reactions of *N7*-(2′-hydroxy-3′,4′-epoxy-but-1′-yl)guanine free bases released during thermal hydrolysis of DEB-treated DNA.[46] In contrast, our attempts to quantify interstrand and intrastrand bis-N7G-BD lesions following their spontaneous hydrolysis at physiological temperature (37 °C) failed to provide reproducible results because of the significant differences in their hydrolytic stability (see below).

Importantly, the relative contribution of intrastrand G−G cross-linking to the total number of bis-N7G-BD adducts was strongly dependent on diepoxide stereochemistry, accounting for 4% of total bis-N7G-BD lesions for *S,S*-DEB, 19% for *R,R*-DEB, and 51% for *meso*-DEB (Table 1). The presence of significant numbers of intrastrand G−G lesions in *meso*-DEB-treated DNA (Table 1) is consistent with the inefficient interstrand adduct formation by this stereoisomer (Figure 2). In contrast, *S,S*-DEB specifically forms interchain G−G cross-links but induces few intrastrand bis-N7G lesions (Figure 2, Table 1). *R,R*-DEB appears to have intermediate cross-linking specificity (Table 1). We propose that the three DEB isomers give rise to similar numbers of N7-(2′-hydroxy-3′,4′-epoxybut-1′-yl)guanine monoadducts, which have different fates in DNA, depending on their stereochemistry (Scheme 3). The epoxy ring of *S,S* monoadducts is subject to an S_N2-type nucleophilic attack

(43) Millard, J. T.; Weidner, M. F.; Kirchner, J. J.; Ribeiro, S.; Hopkins, P. B. *Nucleic Acids Res.* **1991**, *19*, 1885−1891.
(44) Zeng, Y.; Wang, Y. *J. Am. Chem. Soc.* **2004**, *126*, 6552−6553.
(45) Wang, Y.; Taylor, J. S.; Gross, M. L. *Chem. Res. Toxicol.* **1999**, *12*, 1077−1082.
(46) Tretyakova, N. Y.; Sangaiah, R.; Yen, T. Y.; Swenberg, J. A. *Chem. Res. Toxicol.* **1997**, *10*, 779−785.

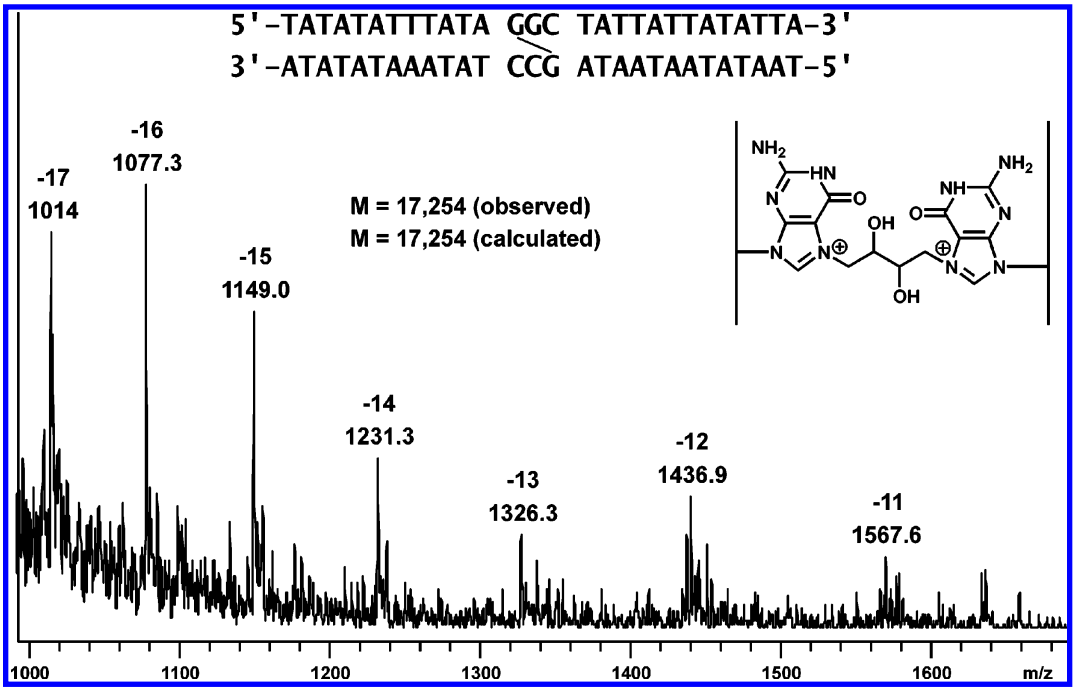

Figure 3. ESI$^-$ mass spectrum of interstrand cross-linked DNA 28-mer (5′-TAT ATA TTT ATA GGC TAT TAT TAT ATT A) (+ strand) extracted from the slowly moving band on denaturing PAGE (Figure 2). The observed molecular weight (M = 17 254) is consistent with the presence of a single bis-N7G-BD cross-link (calculated, M = 17 254).

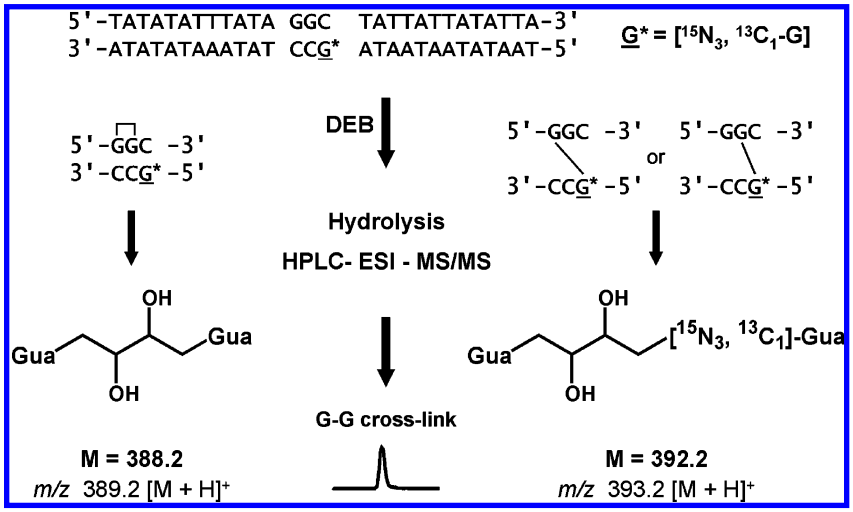

Figure 4. Stable isotope labeling HPLC−ESI$^+$-MS/MS approach to distinguish between intrastrand and interstrand bis-N7G-BD cross-link formation by DEB in 5′-GGC-3′ sequences.

by the N7-guanine in the complementary DNA strand, leading to the preferential formation of interstrand bis-N7G cross-links (Scheme 3). *meso*-DEB derived intermediates similarly participate in nucleophilic substitution by the neighboring N7-guanine in the same DNA strand, giving rise to equal numbers of intrastrand and interstrand bis-N7G-BD lesions (Scheme 3).

DEB-induced interstrand lesions involve distal guanines within 5′-GGC context. In their original publication, Brookes and Lawley proposed that DEB cross-links the opposite DNA strands within 5′GC dinucleotides.[25,47] More recent studies utilizing gel electrophoresis contradict this original hypothesis, suggesting that, in analogy with nitrogen mustards, interstrand cross-linking by DEB involves the distal guanines within 5′GNC context.[28] This sequence preference is perhaps surprising given the fact that a four-carbon chain of DEB (4−5 Å) must span the distance between the N7-guanine atoms in 5′GNC (8.9 Å) and requires considerable conformational flexibility of DNA to accommodate a butanediol linker.

Because gel electrophoresis based studies reported in the literature[28,29] employed very high DEB concentrations (300−1000 mM) and did not examine actual DNA adduct structures, we decided to re-examine sequence preferences for interstrand cross-linking by DEB using a novel, stable isotope labeling based approach. A DNA 28-mer was prepared in which the 5′ guanine in the (+) strand was labeled with $^{15}N_3$,$^{13}C_1$:

5'-d(TAT ATA TTT ATA [$^{15}N_3$,$^{13}C_1$-G] GC TAT TAT TAT ATT A)

3'-d(ATA TAT AAA TAT C CG ATA ATAATA TAA T)

1,3-/1,2-Interstrand cross-linking in this duplex can be distinguished by the molecular weights of the resulting G−G conjugates: 1,3-bis-N7G adducts, but not 1,2-bis-N7G adducts,

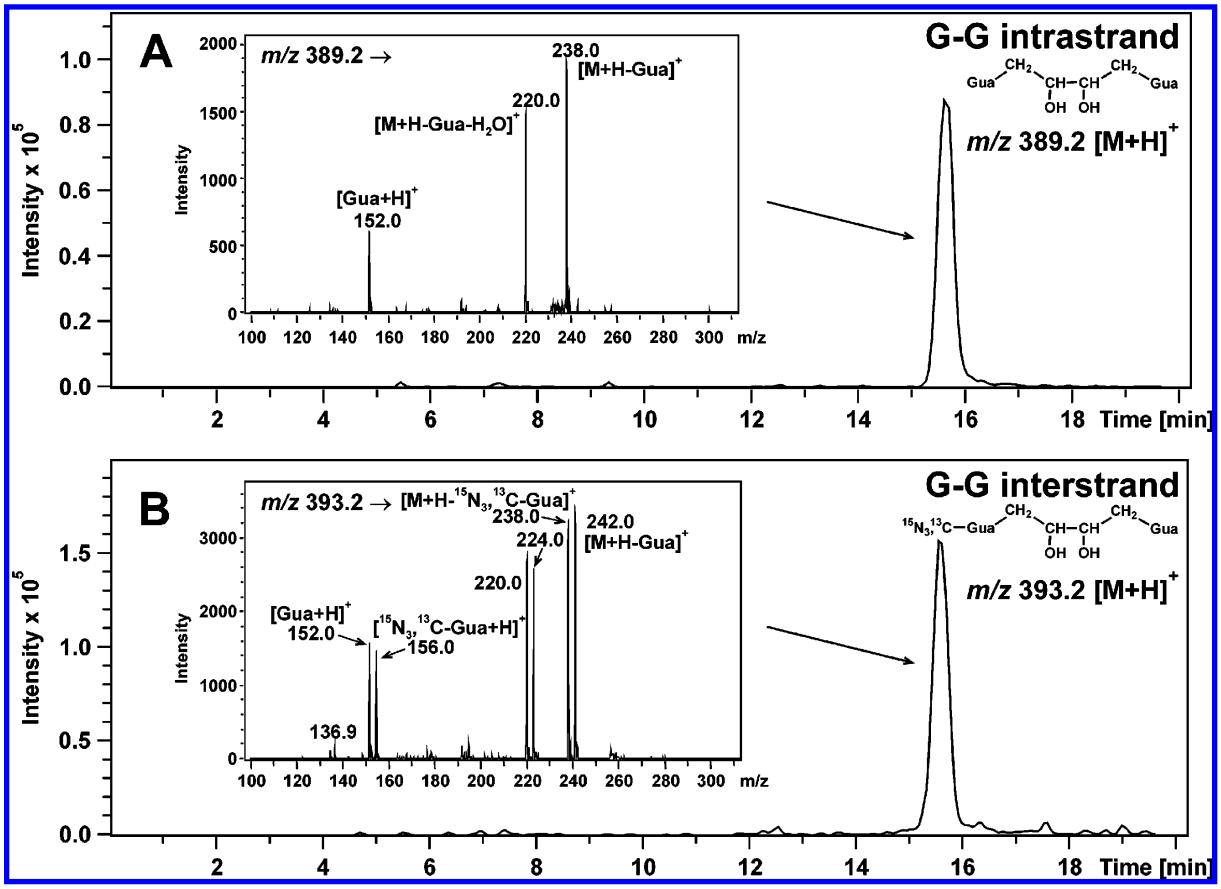

Figure 5. HPLC−ESI+-MS/MS analysis of 1,4-bis-(guan-7-yl)-2,3-butanediol (bis-N7G-BD) adducts in DNA hydrolysates derived from *meso*-DEB-treated duplex (5′-TAT ATA TTT ATA GGC TAT TAT TAT ATT A) (+ strand), (5′-TAA TAT AAT AAT A[1,7,NH_2-$^{15}N_3$-2-^{13}C-G]C CTA TAA ATA TAT A) (− strand). Extracted ion chromatograms corresponding to intrastrand (unlabeled) and interstrand ($^{15}N_3$,$^{13}C_1$-labeled) bis-N7G-BD cross-links were obtained by monitoring the transitions *m/z* 389.2 $[M + H]^+ \rightarrow$ 152.0 $[Gua + H]^+$ and *m/z* 393.2 $[M + H]^+ \rightarrow$ 156.0 $[^{15}N_3{}^{13}C_1\text{-Gua} + H]^+$, 152.0 $[Gua + H]^+$, respectively. Inset: MS/MS spectra corresponding to unlabeled (A) and $^{15}N_3$,$^{13}C_1$-labeled bis-N7G-BD (B).

Table 1. Quantitative Analysis of 1,3-Interstrand, 1,2-Interstrand, and 1,2-Intrastrand 1,4-Bis-(guan-7-yl)-2,3-butanediol Cross-Links Generated in 5′-GGC-3′/3′-CCG-5′ Sequence Context

DEB isomer	Total adduct number, pmol/nmol DNA[a]	% 1,3 interstrand 5′-GGC-3′ / 3′-CCG-5′	% 1,2 interstrand 5′-GGC / 3′-CCG	% 1,2 intrastrand 5′-GGC-3′ / 3′-CCG-5′	Molar ratio interstrand / intrastrand
S,S	3.3 ± 0.4	96	0	4	24
R,R	1.2 ± 0.3	68	13	19	4.2
racemic	2.4 ± 0.2	90	3	7	13
meso	0.8 ± 0.2	49	0	51	0.96

[a] Average ± SD of three measurements. It should be noted that although the total yields of bis-N7G-BD adducts in the 5′GGC sequence differ depending on DEB stereochemistry (Table 1), they are similar in calf thymus DNA (Figure 1). This can be explained by the presence of other potential cross-linking sites (in addition to 5′-GGC) in genomic DNA.

should bear the $^{15}N_3$,$^{13}C_1$ isotope tag. Following incubation with individual DEB stereoisomers, interstrand cross-linked duplexes were isolated by denaturing PAGE. Bis-N7G-BD lesions were quantitatively released by acid hydrolysis, and the molar ratio between 1,3- ([$^{15}N_3$, $^{13}C_1$]-labeled) and 1,2- (unlabeled) interstrand adducts was established from their HPLC−ESI+-MS/MS peak areas (*m/z* 393.2 and 389.2, respectively). We found that, for all three DEB stereoisomers, the majority of interstrand bis-N7G lesions derived from the alkylation of distal guanines on opposite DNA strands of the 5′-GGC sequence (Table 1). Only *R,R*-DEB was capable of inducing 1,2-interstrand lesions (13% of the total number of bis-N7G-BD adducts, Table 1).

1,3-Interstrand cross-linking specificity exhibited by DEB in 5′-[$^{15}N_3$,$^{13}C_1$-G] GC trinucleotides originates from the cross-linking step, rather than from the sequence-dependent formation of monoalkylated intermediates. Indeed, HPLC−MS/MS analysis of N7-THBG lesions in the same samples provides no evidence for the preferential formation of $^{15}N_3$,$^{13}C_1$-labeled N7-THBG (results not shown). We conclude that N7-(2′-hydroxy-3′,4′-epoxybut-1′-yl)-guanine (N7-HEBG) monoadducts are produced in a sequence-independent manner at all guanine bases throughout a DNA duplex and are primarily hydrolyzed to N7-THBG. Only monoadducts produced in a suitable sequence context can give rise to biologically relevant bifunctional lesions (5′-GNC for interstrand cross-linking and 5′-GG for intrastrand cross-linking). In summary, our results confirm common sequence preferences for interstrand DNA cross-linking by DEB and by the antitumor nitrogen mustards[28,48] and reveal further

Scheme 3. Formation of Intrastrand and Interstrand DNA Cross-Linking by DEB Stereoisomers

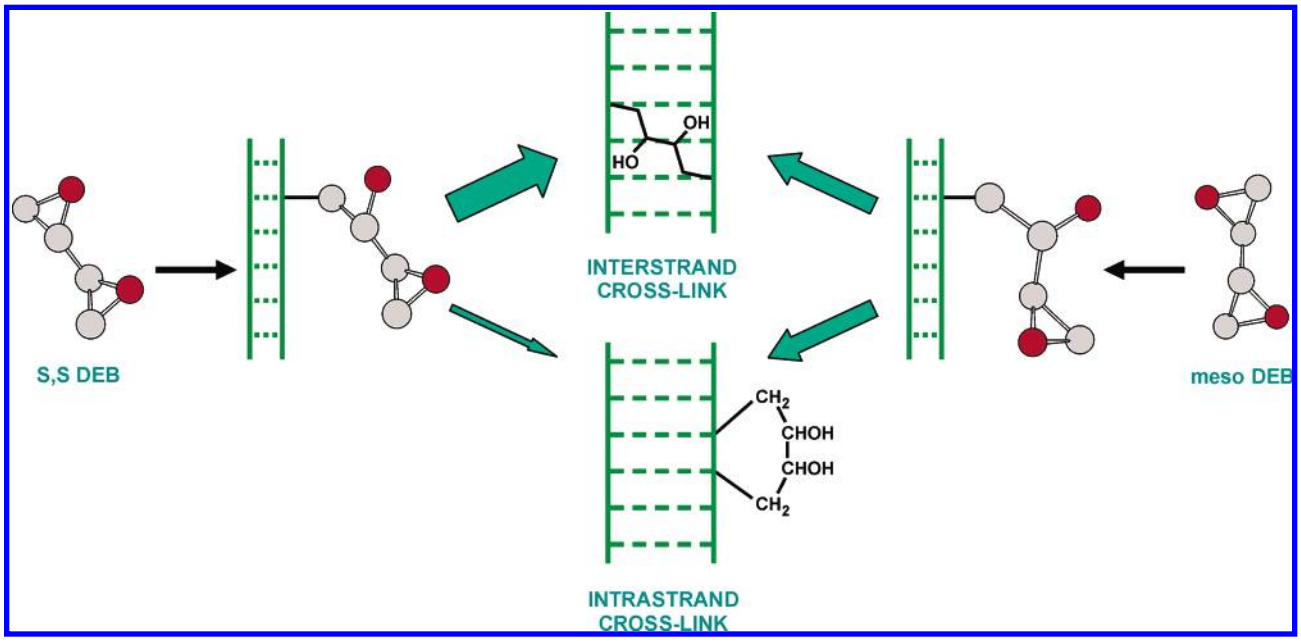

stereospecific differences between DNA−DNA cross-linking by the optical isomers of DEB.

Intrastrand and interstrand bis-N7G-BD lesions have different stabilities in DNA. N-7 alkylation of guanine in DNA generates a positive charge at the modified nitrogens, leading to spontaneous depurination of the adducted nucleobase and the concurrent formation of apurinic sites.[49] We previously reported that bis-N7G-BD lesions are more stable in DNA than the corresponding N7-guanine monoadducts.[27] In the present work, we employed a stable isotope labeling approach to directly compare the hydrolytic stability of intrastrand and interstrand bis-N7G-BD adducts in double-stranded DNA. The DNA 28-mer containing a single 5′-[1,7, NH_2-$^{15}N_3$,2-^{13}C-G]GC-3′/3′-CCG-5′ and 5′-GGC-3′/3′-CC[1,7,NH_2-$^{15}N_3$,2-^{13}C-G]-5′ trinucleotide was treated with *R,R*-DEB to generate both interstrand and intrastrand cross-links (Table 1). DEB-treated DNA was precipitated with cold ethanol, redissolved in buffer, and incubated at physiological conditions. Aliquots were removed at specific times, and the kinetics of the spontaneous release of interstrand and intrastrand bis-N7G-BD nucleobase conjugates from this duplex was determined by HPLC−ESI^+-MS/MS analysis of [$^{15}N_3$,$^{13}C_1$]-bis-N7G-BD and unlabeled bis-N7G-BD, respectively. Another aliquot was completely hydrolyzed to establish the starting numbers of intrastrand and interstrand bis-N7G-BD cross-links in this DNA. First-order kinetic analysis (Figure 6) indicated that the half-life of interstrand N7G−N7G DEB cross-links in double-stranded DNA is 147 h, while the $t_{1/2}$ of intrastrand bis-N7G-BD adducts at the same conditions is 35 h. The experiment was repeated 4 separate times, and the results consistently demonstrated faster hydrolytic release of intrastrand bis-N7G-BD adducts from the DNA backbone. This noticeable difference in stability may be explained by a greater charge density in intrastrand bis-N7G-BD adducts which contain

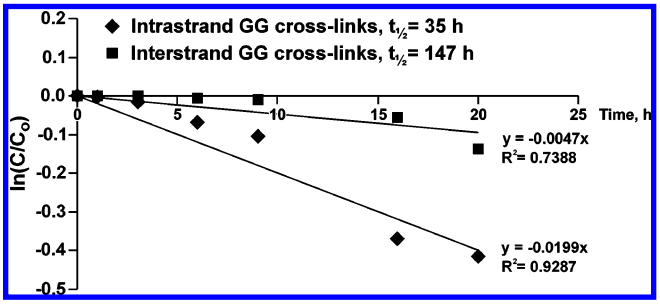

Figure 6. First-order kinetics for spontaneous depurination of intrastrand and interstrand *R,R*-bis-N7G-BD lesions from double-stranded DNA. Bis-N7G-BD adducts were generated by treating $^{15}N_3$,^{13}C-labeled DNA duplex (5′-TAT ATA TTT ATA GGC TAT TAT TAT ATT A) (+ strand) with *R,R*-DEB. DNA was precipitated with cold ethanol and incubated at physiological conditions (37 °C, 200 mM NaCl). The amounts of hydrolytically released intrastrand and interstrand bis-N7G-BD cross-links were determined from HPLC−ESI^+-MS/MS peak areas corresponding to bis-N7G-BD (*m/z* 389.2→ 238.0) and [$^{15}N_3$]-bis-N7G-BD (*m/z* 393.2 → 242.0), respectively.

two neighboring, positively charged N7-guanine adducts.[50] For example, Wogan and coauthors observed a decreased stability of the N7-guanine adducts of aflatoxin in DNA that had a higher number of adducts per DNA base pair.[51] In contrast, N7-alkylguanines within 1,3-interstrand bis-N7G-BD lesions are located in different DNA strands and are flanked by another base pair, decreasing the "adduct density" as compared with the corresponding 1,2-instrastrand lesions. Alternatively, the presence of a neighboring abasic site may facilitate the second hydrolytic step because of an increased solvent accessibility of the partially depurinated DNA strand.

Discussion

Our results presented above indicate that chirality can be an important factor in determining DNA−DNA cross-linking specificity of bifunctional electrophiles. We found that bifunc-

(47) Brookes, P.; Lawley, P. D. *J. Chem. Soc.* **1961**, 3923−3927.
(48) Rink, S. M.; Solomon, M. S.; Taylor, M. J.; Rajur, S. B.; McLaughlin, L. W.; Hopkins, P. B. *J. Am. Chem. Soc.* **1993**, *115*, 2551−2557.
(49) Singer, B.; Grunberger, D. *Molecular Biology of Mutagens and Carcinogens*; Plenum Press: New York and London, 1983.
(50) Gates, K. S.; Nooner, T.; Dutta, S. *Chem. Res. Toxicol.* **2004**, *17*, 839−856.
(51) Groopman, J. D.; Croy, R. G.; Wogan, G. N. *Proc. Natl. Acad. Sci. U.S.A* **1981**, *78*, 5445−5449.

tional DNA alkylation by *S,S*-DEB within the 5′-GGC target sequence produced almost exclusively 1,3-interstrand bis-N7G-BD lesions, while *meso*-DEB gave rise to similar numbers of interstrand and instrastrand bis-N7G adducts (Table 1). *R,R*-DEB exhibited intermediate specificity but was the only isomer to induce a significant number of 1,2-interstrand cross-links (Table 1). Although 1,2-intrastrand cross-linking by DEB has been previously hypothesized,[4] our experiments provide the first direct evidence for the formation of such lesions in DEB-treated DNA. The relative contribution of intrastrand DNA alkylation by DEB in genomic DNA is likely to be greater than that in 5′GGC trinucleotides examined here because of the statistically higher frequency of 5′-GG dinucleotides in general DNA sequences.

Interchain DNA−DNA cross-linking by therapeutic bifunctional alkylating agents is considered the primary mechanism for their antitumor activity, while intrastrand lesions can exhibit both cytotoxic and promutagenic properties.[1,4] Interstrand DNA−DNA adducts are among the most toxic nucleobase lesions because they inhibit DNA replication and transcription, and their enzymatic removal in cells is problematic because of the loss of template information in both DNA strands. This requires a complex repair process usually involving both nucleotide excision repair and recombination repair,[52] which can lead to DNA rearrangements and deletions.[53] Therefore, the preferential formation of interstrand DNA−DNA lesions by *S,S*-DEB is consistent with its potent cytotoxicity and its ability to induce chromosomal aberrations.[15] On the other hand, intrastrand bis-alkylation of DNA by *meso*-DEB is likely to play a role in mutagenesis.[4] Importantly, our recent HPLC−ESI-MS/MS results for bis-N7G-BD in liver DNA of laboratory animals exposed to the metabolic precursor of DEB, 1,3-butadiene, provide evidence for the formation of both diastereomers of bis-N7G-BD in vivo (Loeber and Tretyakova, manuscript in preparation).

The observed differences between the ability of DEB isomers to induce DNA−DNA lesions are likely caused by different orientations of functional groups in stereoisomeric N7-(2′-hydroxy-3′,4′-epoxybut-1′-yl)-guanine (N7-HEBG) intermediates (Scheme 3). In *S,S*- and *R,R*-N7-HEBG, the epoxy ring and the 2′-hydroxy group reside on one side of the plane formed by the carbon chain, while, in the *meso* isomer, the epoxy oxygen and the 2′-OH are located on different sides of the plane (Scheme 3), potentially influencing the site of the second alkylation. A recent NMR study of N^6-(2′,3′,4′-trihydroxybut-1′-yl)-deoxyadenosyl adducts has revealed distinct stereospecific interactions between the hydroxyl groups of the trihydroxybutyl side chain and the neighboring nucleobases.[54] In the *S,S* adduct, hydrogen bond formation was observed between the β-OH of the side chain and the O4 of thymine in the opposite strand, while, for the *R,R* adduct, hydrogen bonding was formed between the γ-OH and the thymine O4 in the opposite DNA strand.[54] Although no NMR data is currently available for stereoisomeric N7-HEBG intermediates, examination of molecular models suggests that hydrogen bonding between the 2′-hydroxy group in *S,S*- and *R,R*-N7-HEBG and the N-3 of the 3′-neighboring guanine may position the 3′,4′-oxirane ring in a favorable orientation for the S_N2-type nucleophilic attack by the N-7-guanine in the opposite strand (Figures S-5 and S-6). In contrast, hydrogen bonding between the 2′-hydroxyl and 3′-neighboring guanine in *meso*-DEB-induced *S,R* and *R,S* epoxy alcohol intermediates stabilizes the conformation in which the oxirane oxygen faces the N7-guanine in the opposite strand (e.g., Figure S-7). As a result, S_N2 attack by the 3′-neighboring guanine is preferred, shifting the cross-linking ratio in favor of intrastrand lesions (Scheme 3).

Our stable isotope labeling experiments confirm the preferential formation of interstrand G−G butanediol lesions of DEB between the guanine bases two residues apart in the DNA duplex (1,3-*cross*-linking), with only the *R,R* isomer inducing measurable numbers of 1,2-interstrand lesions (Table 1). These results are in agreement with an earlier study by Millard et al.[28] who used hot piperidine cleavage to reveal the alkylation sites within DNA duplexes treated with racemic DEB. Further theoretical and structural studies are needed to help explain this unusual sequence specificity. The distance between the N7-guanine atoms in 5′-GNC sequences of B-DNA (8.9 Å) is several angstroms too long as compared with the length of the four-atom tether of DEB. It is possible that the initially formed cationic N7-(2′-hydroxy-3′,4′-epoxybut-1′-yl)-guanine intermediates (Figures S5-8) induce a conformational change in DNA, bringing the second epoxide closer to the target G for interstrand cross-link formation.[55,56] Alternatively, the formation of N7−HEBG may alter the chemical reactivity of neighboring guanine bases via electronic or structural mechanisms, making the nucleophilic attack by the distal G more favorable. Irrespective of the mechanism, the resulting 1,3-bis-N7G-BD lesions must distort the DNA duplex in order to be accommodated. Indeed, our exonuclease resistance studies show that the 3′-exonuclease activity of *E. coli* Polymerase I is blocked one nucleotide ahead of the interstrand bis-N7G-BD lesion, suggesting that the DNA duplex undergoes a structural change in the vicinity of the cross-link (Figure S-9, S-10). This local distortion of the DNA duplex may serve as a recognition signal for proteins involved in cross-link repair. Studies are now underway to analyze the structural perturbations induced by N7-(2′-hydroxy-3′,4′-epoxybut-1′-yl)-guanine lesions and to examine the biological processing of intrastrand and interstrand bis-N7G-BD lesions in the presence of DNA polymerases and DNA repair proteins.

Acknowledgment. We thank Ms. Colleen Murray (University of Minnesota) for her help with generating molecular models of DNA duplexes containing stereoisomeric N7-(2′-hydroxy-3′,4′-epoxybut-1′-yl)-guanine adducts and bis-N7G-BD cross-links, Prof. Yusuf Abul-Hajj (University of Minnesota Department of Medicinal Chemistry) for critical review of the manuscript, and Gregory Janis for editorial help. Funding for this research was from the Leukemia Research Foundation and a grant from the National Cancer Institute (CA-100670). Rachel Loeber is supported by an NIH Chemistry-Biology Interface Training grant (T32-GM08700).

Supporting Information Available: Synthesis of *R,R*-, *S,S*-, and *meso*-DEB (S-1); proton NMR spectra of synthetic DEB

(52) Cole, R. S. *Proc. Natl. Acad. Sci. U.S.A.* **1973**, *70*, 1064−1068.
(53) Zheng, H.; Wang, X.; Warren, A. J.; Legerski, R. J.; Nairn, R. S.; Hamilton, J. W.; Li, L. *Mol. Cell Biol.* **2003**, *23*, 754−761.
(54) Merritt, W. K.; Scholdberg, T. A.; Nechev, L. V.; Harris, T. M.; Harris, C. M.; Lloyd, R. S.; Stone, M. P. *Chem. Res. Toxicol.* **2004**, *17*, 1007−1019.
(55) Fan, Y.-H.; Gold, B. *J. Am. Chem. Soc.* **1999**, *121*, 11942−11946.
(56) Remias, M. G.; Lee, C. S.; Haworth, I. S. *J. Biomol. Struct. Dyn.* **1995**, *12*, 911−936.

stereoisomers (S-2), GC−MS traces or *R*,*R*-, *S*,*S*-, and *meso*-DEB (S-3); HPLC−ESI$^+$ MS/MS methods for bis-N7G-BD diastereomers (S-4); molecular models of stereoisomeric N7-(2′-hydroxy-3′,4′-epoxybut-1′-yl)-guanine adducts in 5′-GGC trinucleotides (S-5−8), and exonuclease blockage sites in a duplex containing racemic 1,4-bis-(guan-7-yl)-2,3-butanediol cross-link (S-9, S-10). This material is available free of charge via the Internet at http://pubs.acs.org.

JA051979X